Heliyon 10 (2024) e38071

Contents lists available at ScienceDirect

Heliyon

journal homepage: www.cell.com/heliyon

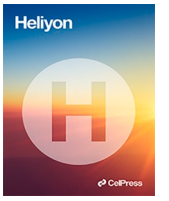

Research article

Hybrid fibrous architectures-mediated gene transfer by pDNA nanoparticles into macrophages

Jana Ghitman [a,b], Gratiela Gradisteanu Pircalabioru [b,c], Calin Deleanu [d], Eugeniu Vasile [e], Ciprian Iliescu [b,f,g], Horia Iovu [a,b,f,*]

[a] *Advanced Polymer Materials Group, National University of Science and Technology Politehnica Bucharest, 1-7 Gh. Polizu Street, 011061, Bucharest, Romania*
[b] *Center of Excellence in Bioengineering – eBio-hub, National University of Science and Technology Politehnica Bucharest - CAMPUS, 6 Iuliu Maniu Boulevard, 061344, Bucharest, Romania*
[c] *Research Institute of the University of Bucharest (ICUB), University of Bucharest, 91-95 Splaiul Independentei, 050095, Bucharest, Romania*
[d] *"C. D. Nenitescu" Institute of Organic and Supramolecular Chemistry, 202B Splaiul Independentei, 060023 Bucharest, Romania*
[e] *Department of Oxide Materials Science and Engineering, National University of Science and Technology Politehnica Bucharest, 1-7 Gh. Polizu, 060042, Bucharest, Romania*
[f] *Academy of Romanian Scientists, 54 Splaiul Independentei, 050094, Bucharest, Romania*
[g] *National Research and Development Institute in Microtechnologies—IMT Bucharest, 126A Erou Iancu Nicolae Street, 077190, Voluntari, Romania*

ARTICLE INFO

Keywords:
Macrophages
Hybrid electrospun architecture
Transient gene transfection
PEI/pDNA nanoparticles

ABSTRACT

Gene therapy is one of the most potential therapeutic approaches in direct and specific regulation of biological functions of macrophages at the gene level for efficient cell therapy. However, the delivery of genetic material to macrophages is extremely challenging, because of low stability, specificity and inability of therapeutic genes to efficiently enter the cells. Here, we present a method that uses the hybrid electrospun architectures based on gelatin-alginate decorated with carboxylated graphene oxide (HAG/G) as efficient substrate for loading and *in vitro* local and controlled delivery of plasmid DNA (pDNA) to macrophages as an alternative to systemic gene delivery carriers. Polyethyleneimine (PEI) is employed to assemble PEI/pDNA nanoparticles (Np) - used as model of carrier. The dispersion of GO-COOH sheets shifts the surface zeta potential of HAG/G to high negative value (SZP = −16.8 ± 2.21 mV) and further increases the encapsulation efficiency of PEI/pDNA Np onto hybrid HAG/G electrospun architectures to ~ 69 % (HAG/G-Np). The *in vitro* biological investigations show a good metabolic activity of macrophages seeded onto HAG/G-Np (MTT assay), while gene expression experiments (fluorescent microscopy) show a 30 % increase in transient gene transfection of cells cultured in the presence of HAG/G-Np as compared to those incubated with free PEI/pDNA Np.

1. Introduction

Cell and gene therapy represents one of the latest advancements in biomedical technology, which revolutionized the medical field by offering cutting-edge treatments for a wide range of diseases. According to BCC Research Study the global cell and gene therapy

* Corresponding author. Advanced Polymer Materials Group, National University of Science and Technology Politehnica Bucharest, 1-7 Gh. Polizu Street, 011061, Bucharest, Romania.
E-mail address: horia.iovu@upb.ro (H. Iovu).

https://doi.org/10.1016/j.heliyon.2024.e38071
Received 2 April 2024; Received in revised form 11 September 2024; Accepted 17 September 2024
Available online 25 September 2024

market was evaluated at USD 19,978 million in 2022 and is estimated to reach $23.3 billion through 2028 [1].

Gene therapy is the modulation of gene expression in particular cells by introducing exogenous genetic material to treat pathological conditions [2,3]. The mainstay factor in utilizing the full potential of gene therapy technology represents the design of suitable gene carrier capable of delivering efficiently the therapeutic gene to the targeted cell/tissue, facilitating intracellular trafficking. The packaging of therapeutic genes in a nanocarrier, using viral or non-viral vectors is highly desirable both to protect the therapeutic gene from degradation and to deliver it into the target cells [4,5]. Today, viral vectors (e.g., adenovirus, retrovirus, adeno-associated virus, etc.) are the most clinically advanced gene delivery assets, owing to their ability to penetrate unassisted cells, high specificity and efficacy. However, challenges related to strong immunogenicity, safety and formulation complexity still are important concerns [6,7].

Besides viral vectors, lipid nanoparticles (LNPs) and extracellular vesicles (EVs) are esteemed as efficient and secure approaches to deliver the therapeutic gene to the site of action. Different formulations of lipid nanoparticles have been investigated as gene carriers [8,9] for the treatment of various diseases (e.g., virus infections, cancer, genetic diseases) [10,11], successfully entering the clinic for the delivery of siRNA [12] and mRNA [13], marking a milestone for mRNA therapeutics [11]. Extracellular vesicles (EVs) represent a class of specific protein-decorated phospholipid particles (e.g., exosomes, microvesicles, and apoptotic bodies) [14] produced by cells, which are involved in many (patho)physiological processes [15,16]. Owing to their uniqueness in biology and function (e.g., biocompatibility, cargo loading capacity, deep tissue penetration [17] and versatility in loading therapeutics payloads [18] the EVs represent also an active and important line of research in gene therapy. Considering that EVs can constitute a new system of cell–cell communication [15], these have been used as safe and accurate transport vectors for genes such as siRNA, mRNA, pDNa or CRISPR/CAS9 in different therapies (e.g., anti-inflammatory, anticancer, cardiovascular and pulmonary therapies) [14,19], as alternative to conventional synthetic carriers.

Interpolyelectrolyte complexes between polyelectrolytes and nucleic acids represent other non-viral strategies with particular importance in the gene delivery field. Polyethylene imide (PEI) remains the "gold standard" in non-viral transfection of mammalian cells both *in vitro* and *in vivo* [2]. Containing a particular arrangement of amino functionalities, PEI is endowed with a notable cationic charge density (at reduced pH values) and buffering capacity, which beside efficient DNA complexation is capable to promote the endosomal escape *via* the "proton-sponge" effect [20]. However, systemic injection may generate risks of gene expression in non-targeted/normal cells, reducing therapeutic efficacy, which is still low as compared to viral vectors [21].

Macrophages are innate immune cells with crucial role in sustaining a balanced response to homeostatic or tissue-damaging indicators [22]. These cells, strategically distributed throughout the body [23], are highly heterogeneous and can rapidly change their function (protective or pathogenic), in response to local microenvironmental signals [23,24].

The controllable activation of macrophages towards desirable phenotypes *in vivo* and *in vitro* may provide effective treatments for a number of inflammatory and proliferative diseases and have attracted considerable attention as targets for the treatment of diseases of

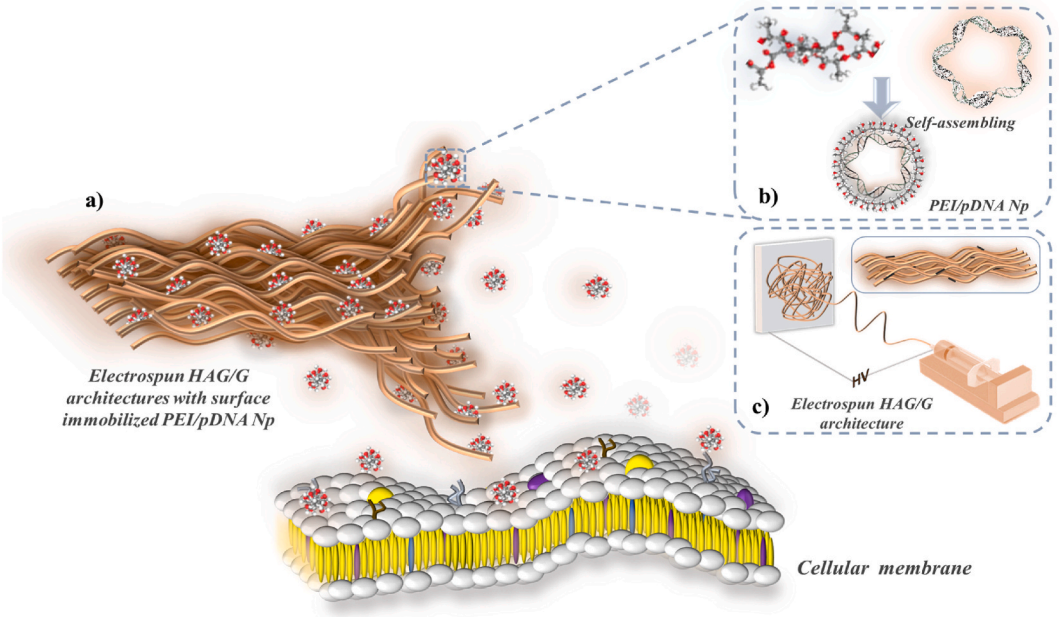

Fig. 1. Schematic for the components and application of the hybrid HAG/G-Np model as local and efficient gene delivery system: **a)** – General concept and *in vitro* application of HAG/G electrospun architectures with surface immobilized PEI/pDNA Np. After applying HAG/G Np, the PEI/pDNA can be locally released in a controllable manner through the biodegradation of hybrid HAG/G fibrous architecture; **b)** – Complexation of PEI (polyethylene imine) with pDNA (plasmid-DNA) to achieve robust self-assembled PEI/pDNA Np. Freshly prepared PEI/pDNA Np can be immobilized on the surface of stabilized electrospun HAG/G architectures through non-covalent interactions, mainly involving charge attraction forces; **c)** - Fabrication of hybrid HAG/G electrospun architecture.

various etiology [24,25].

Despite the advancements in gene delivery field, most of the gene integration approaches for macrophages regulation fail to meet efficiency targets firstly, being administrated through systemic route, the off-target effects are inevitable [26], secondly because of the phagocytic properties of macrophages and the membrane barriers that limit their entry into cells [27]. At the same time, it is known that the systemic delivery of free therapeutic gene hardly can reach the target cells/tissue because of its premature degradation by endonucleases in biological fluids, extracellular matrix and inefficient cellular internalization [2]. Kawabata et al. [28] have estimated that the half-life of naked plasmid DNA (pDNA) is approximately 10 min following intravenous injection in mice. Mahor et al. [29] have reported targeted gene delivery to RAW 264.7 macrophages using mannosylated polyethylenimine-hyaluronan nanohybrids as gene carrier with transfection efficiency only up to ~7.5 %, while Zhang and co-workers [30] have managed to improve the transfection performance to ~ 10 % in the same cell line by formulating mannose or folate functionalized star polymers as gene carriers. Thus, the development of efficient gene delivery approaches overcoming the problems related to reduced specificity and phagocytosis processes, are timely for macrophage-targeted gene therapy.

In this scenario, here we report a biodegradable hybrid gelatin-alginate electrospun architecture decorated with carboxylated graphene oxide (HAG/G) as versatile substrate for local and controlled delivery of PEI/pDNA nanoparticles (Np) to macrophages an alternative to systemic gene delivery carriers (Fig. 1). The PEI/pDNA Np are used as model of carriers and are immobilization on the surface of scaffolds. In fact, the integration of gene carriers with rationally designed fibrous architecture with graphene layers distributed along the nanometric size of fibers may act as spatial substrate for loaded nanoparticles. The amount of PEI/pDNA Np immobilized on the surface of hybrid HAG/G fibrous architecture can be fine-tuned through modulating the amount of carboxylated graphene oxide (GO-COOH). Using pDNA encoding green fluorescent protein - GFP as model cargo, we have investigated the cytocompatibility, gene transfection efficiency and immunomodulatory activity of PEI/pDNA immobilized onto hybrid HAG/G electrospun architectures (HAG/G-Np) in macrophage cells cultured *in vitro*. The *ex vivo* genetically activated macrophages and then reintroduced into the body could be used to deliver the therapeutic gene into the diseased tissues [31].

2. Materials and methods

2.1. Materials

Linear Polyethylene imine with Mw = 10k Da (PEI), Gelatin from cold water fish skin (Gel), Sodium Alginate from brown algae (Alg), Polyethylene oxide with Mw = 600 KDa (PEO), 4-(1,1,3,3-tetramethylbutyl) phenyl-polyethylene glycol (Triton-X), Glutaraldehyde (GA), Trizma base with Mw = 121.14 g/mol and $CaCl_2$ were supplied from Sigma-Aldrich Chemie GmbH, Germany; carboxylated graphene oxide (GO-COOH) was provided by NanoInnova Technology; plasmid DNA (pVectOZ-GFP, 5757 bp) from OZ Bioscience, France.

3. Methods

3.1. Fabrication of hybrid HAG and HAG/G fibrous architectures

The hybrid gelatin-alginate (HAG) and gelatin-alginate electrospun architecture decorated with carboxylated graphene oxide (HAG/G) were formulated following the protocol described in our previous work [32]. The hybrid HAG/G electrospun architectures were fabricate from a precursor system consisting of 0.1 wt% GO-COOH dispersed into 0.5 wt% Triton-X aqueous solution, followed by the solubilization of PEO (4 wt%) and addition of Alg (4 wt%) and Gel (40 wt%) solutions in a ratio of 2/1/2 (v/v/v). The hybrid HAG electrospun architectures were formulated using the same protocol, except the dispersion of GO-COOH layers. The electrospinning process was carried out using climate-controlled electrospinning equipment (IME Technologies, Netherlands) followed by the two-step crosslinking process, generating interpenetrated hybrid networks. The crosslinking step along with the comprehensive structural, morphological and biological characterization of the formulated hybrid electrospun architectures were reported [32].

3.2. Physicochemical characterization

The morphology of hybrid HAG and HAG/G electrospun scaffolds were observed under the scanning electron microscope (SEM, Quanta Inspect F50, USA) supplied with a field-emission electron beam gun (FEG) with 1.2 nm resolution. The micrographs were captured with an emission gun operated at 30 kV. The surface wettability of hybrid fibrous architectures was investigated by sessile drop method using Kruss DSA100S instrument (Germany), equipped with a CF03 digital camera. The *in vitro* degradation studies were performed in phosphate-buffer saline (PBS, pH 7.4); the samples were cut in rectangles (10 mm × 10 mm), placed in PBS with or without collagenase (0.03U/mL) and incubated at 37 °C. At predetermined times points (6 h, 12 h, 24 h, 48 h, 72 h) the samples were taken out from the solution, washed with distilled water, dried and weighed, while every 24th hours the immersion medium was replaced with another fresh one. The degree of degradation was calculated using the formula:

$$Weight\ loss\% = \frac{W_0 - W_t}{W_0}\ x\ 100$$

where W_0 represents the initial dry weight and W_t is the dry weight after degradation.

The Surface Zeta Potential (SZP) was measured by Zetasizer Nano ZS, Malvern Instrument, UK, using the Surface Zeta Potential Cell Kit (ZEN1020, Zetasizer, Malvern) and deionized water as dispersing medium of polyethylene (PEG) tracer particles with 0.5 μm diameter. The hybrid HAG and HAG/G scaffolds were cut into rectangles (4 mm × 4 mm) and fixed to the sample holder (situated between the two electrodes) which was subsequently submerged in the aqueous solution containing a specific concentration of PEG tracer particles (d = 500 nm) and ensuring that no air bubble was trapped under the film. The measurement of apparent tracer mobility at different distances from the sample surface was done at 25 °C by setting the size of step to 125 μm (which correspond to ¼ turn of the cell top counterclockwise) and performing three measurements with 10 automatic runs at each step. The SZP of investigated sample was calculated from the plot of reported zeta potential of tracer particles as a function of displacement from the sample surface.

3.3. Assembling and characterization of PEI/pDNA complexes

The PEI/pDNA nanoparticles (Np) were prepared at different N/P molar ratios by adding dropwise different amounts of PEI solution (1 mg/mL, 10 mM Trizma buffer, pH 7.4) into a dilute pDNA solution (0.05 mg/mL, 10 mM Trizma buffer, pH 7.4) under vortex mixing, following by the incubation for 30 min at room temperature before further use. It is important to mention that N/P ratio is defined as the molar ratio of the nitrogen atoms in PEI to the phosphorus atoms of pDNA in the solution mixture and not the N/P ration inside each nanoparticle [33].

The mean hydrodynamic size (Z-ave), polydispersity (PdI) and zeta potential (ζ) of PEI/pDNA Np were studied by Dynamic Light Scattering method using Zetasizer Nano ZS, Malvern Instrument, UK equipped with a He/Ne laser operating at λ = 632 nm. The Z-ave and PdI measurements were performed at a scattering angle of 173° using the low volume cuvettes (ZEN0040, Malvern Instrument) with~200 μL of freshly prepared samples. The samples were equilibrated for 120 s at 25 °C in the instrument and three measurements with 15 automatic successive cycles were run for each specimen. The electrophoretic mobility investigations (converted in zeta potentials by the Henry's equation [34]) were carried out at a detection angle of 13°, using folded capillary cells with inbuilt electrodes at each head (DTS1070, Malvern Instrument). The reported ζ-potentials represent the averaged results of three measurements with 30 automatic successive cycles run at 25 °C. The morphological investigations were performed by a high-resolution transmission electron microscope (HR-TEM, TECNAI F30 G^2 S-TWIN instrument, Hillsboro, OR, USA). A small amount of each sample was deposited on a TEM copper grid covered with a thin amorphous carbon film and subjected to morphology evaluations.

3.4. Immobilization of PEI/pDNA Np on the surface of electrospun hybrid architectures

The PEI/pDNA Np were immobilized on the surface of crosslinked hybrid HAG and HAG/G electrospun scaffolds through physical adsorption method. The freshly assembled PEI/pDNA Np (N/P = 4) were placed 1 mL per well and incubated for 2 h under ambient conditions in the presence of hybrid HAG and HAG/G electrospun scaffolds to allow their adherence to the surface. The morphology of hybrid fibrous architectures with PEI/pDNA Np immobilized on the surface (HAG-Np and HAG/G-Np) was examined under SEM (SEM, Quanta Inspect F50, USA). Further, SYBR Green dye (Thermo Fisher Scientific) was employed to determine the amount of immobilized nanoparticles on the surface of hybrid fibrous architectures. The HAG-Np and HAG/G-Np were mixed with SYBR Green dye solution (5 μg/mL), and the fluorescence was measured at λ_{EX}: 497 nm and λ_{EM}:520 nm on a Flex Station 3 instrument. A calibration curve with known concentrations of pDNA was constructed to convert the readings from the mats into pDNA concentration. The percentage of encapsulation efficiency was calculated using the formula:

$$EE\,\% = \frac{\text{Amount of pDNA in scaffolds}}{\text{Amount of pDNA added in the solution}}\ x\,100$$

3.5. Cell culture

The RAW 264.7 murine macrophages (ATCC) were cultured at a cell density 1 × 10^5/mL cells in Dulbecco's Modified Eagle's medium (DMEM) supplemented with 10 % fetal bovine serum (FBS) and 1 % penicillin-streptomycin at 37 °C in a 5 % CO_2 atmosphere for 24 h to allow the cells attachment. All cell-based experiments were performed by using sterilized samples. The unmodified or PEI/pDNA immobilized hybrid HAG and HAG/G fibrous architectures were cut into 1 mm^2 squares and used for all cell culture experiments. The cells were seeded onto the scaffolds and were incubated in the same conditions for different times, depending on the type of experiment. PEI/pDNA solutions were used at a 1/10 ratio. The cells were seeded onto the scaffolds and were incubated in the same conditions for different times, depending on the type of experiment.

Cell viability and proliferation potential of all samples were evaluated using 3-[4,5-dimethylthiazole-2-yl]-2,5-diphenyltetrazolium bromide (MTT) assay after 24 h and 72 h of culture. Each sample was incubated with 1 mg/mL MTT solution for 4 h at 37 °C and the absorbance at 550 nm was measured by Flex Station 3 spectrophotometer. The percentage of cell viability was calculated using the formula:

$$\textit{Cell viability}\,\% = \frac{OD_{550}\ \text{treated cells}}{OD_{550}\ \text{contol}}\ x\,100$$

The cytotoxic potential was evaluated by LDH assay using Tox-7-KT kit, following the manufacturer's protocol. The samples were incubated for 20 min in darkness, then were spectrophotometrically measured at 490 nm, the cytotoxicity was calculated by the formula [35].

$$Cytotoxicity\ \% = \frac{OD_{490}\ \text{LDH released by the compound tested}}{OD_{490}\ \text{total LDH released by the cells lysed with 5\%Triton} - \text{X}}\ x\,100$$

3.6. Transient gene expression

The transient gene expression efficiency of PEI/pDNA complexes immobilized on the surface of hybrid HAG and HAG/G fibrous architectures were analyzed by fluorescence spectrophotometry and microscopy after 24 h of incubation with RAW 264.7 murine macrophage cells. Then cells were washed three times with PBS, stained with DAPI (2 μg/mL) and visualized under an Olympus IX71 fluorescence microscope (Tokyo, Japan) for qualitative analyses, while for quantitative GFP expression, the cells were trypsinised, washed with PBS and their fluorescence was measured on a Flex station 3 instrument (ex 497 nm, emission 520 nm).

3.7. Immunomodulatory activity (ELISA assay)

The RAW 264.7 macrophages were incubated in the presence of investigated samples for 24 h. The macrophages stimulated in the presence of *E. coli* and those cultivated in standard conditions were used as controls. The supernatant of each sample was collected, and the levels of pro-inflammatory IL-6 and anti-inflammatory IL-10 were quantified using ELISA (Thermo Scientific) following the manufacturer's instructions. Cytokine levels were expressed as pg/mL.

3.8. Statistical analyses

The results were presented as mean ± SD. Statistical comparison was performed by ANOVA tests using GraphPad Prism version 8.0.1, and it was considered significant if $p < 0.05$.

4. Results and discussion

It is well documented that rationally designed electrospun fibrous architectures represent insurmountable gene delivery templates, capable to ensure not only the appropriate guidance and mechanical support for cells development but also may modulate the release

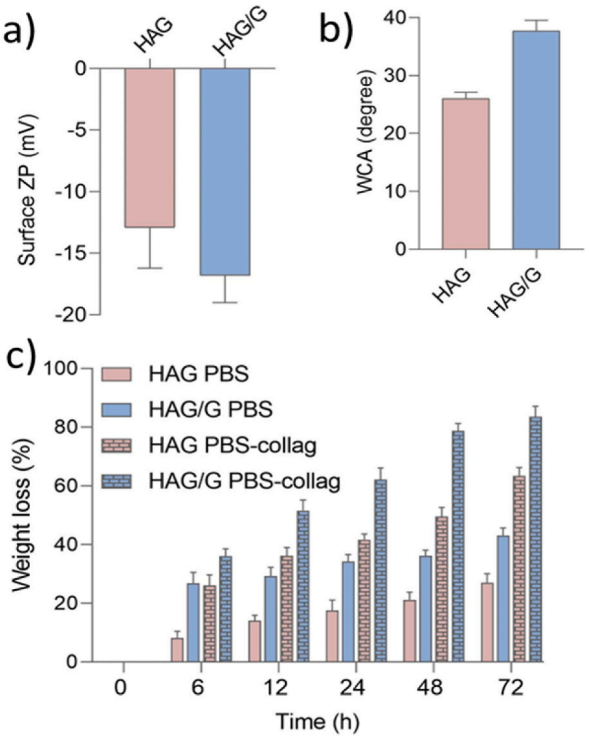

Fig. 2. Physical characterization of hybrid fibrous architectures: **a)** - Surface Zeta Potential (SZP) of hybrid HAG and HAG/G electrospun architectures. The dispersion of GO-COOH sheets shifts the SZP of HAG/G to higher negative value, which may promote the immobilization of positively charged PEI/pDNA Np on its surface; **b)** – Water contact angle (WCA) of hybrid HAG and HAG/G fibrous architectures; **c)** – Weight loss percentage of hybrid HAG and HAG/G fibrous architectures in PBS and PBS with 0.03U/mL collagenase. The dispersion of GO-COOH sheets accelerates the degradation rate of HAG/G in both investigated media.

profile of loaded cargo, in accordance with therapeutic purpose [36]. Previously we have formulated bioinspired GO-COOH decorated hybrid electrospun scaffolds with appropriate features for tissue regeneration, by rationally combining the biomimicry and biocompatibility of two biobased-derived polymers (gelatin and alginate) with carboxylated graphene oxide (GO-COOH) [28]. In this respect, we have formulated bicomponent electrospun alginate-gelatin hybrid scaffolds decorated with two concentrations of GO-COOH (0.1 wt% and 0.2 wt%). Based on the structural, morphological and biological results, the hybrid bicomponent electrospun scaffolds decorated with 0.1 wt% GO-COOH (HAG/G) were used in the present paper and investigated as substrate for *in vitro* local and efficient delivery of PEI/pDNA Np. To evaluate the contribution of GO-COOH sheets in defining the delivery performances of HAG/G, the hybrid alginate-gelatin counterparts (HAG) were also investigated.

The surface properties of artificial biomaterials (e.g., surface charge, surface functional groups, hydrophilicity, and topography) are among the underlying factors toward the successful biomaterial integration and cellular/tissue colonization after being implanted into biological environment, regulating cell behavior, modulating their adhesion, proliferation and signaling [37]. In this framework, surface zeta potential (SZP) represents a relevant parameter in describing the surface charge of biomaterials in contact with a liquid. It must be mentioned that the SZP is impacted by environmental conditions that dictate the protonation or ionization of the intrinsic functionalities of the biomaterial's surface upon contact with the liquid [38]. Here the surface potential of HAG fibrous architecture is originated from the intrinsic functionalities of polysaccharide and protein structure (SZP = -12.9 ± 3.31 mV), while the dispersion of GO-COOH sheets shifts the SZP of HAG/G to higher negative value (-16.8 ± 2.21 mV) (Fig. 2, a) owing to the addition of supplementary negatively charged oxygen containing functionalities (i.e., carboxyl (-COO^-) and hydroxyl (-OH)). The more negative surface zeta potential of hybrid HAG/G fibrous architectures is also in line with the previous quantitative atomic surface composition investigation (XPS), which showed an increased in oxygen content of hybrid electrospun scaffolds following the GO-COOH dispersion [32]. Since the nanoparticles immobilization onto the fibrous architectures is driven by physical absorption process, mainly involving the electrostatic interactions, we expect the immobilization of higher amount of positively charged PEI/pDNA Np on the more negative surface of hybrid HAG/G fibrous architectures as compared to the HAG counterparts.

Beside the SZP, surface wettability is another key parameter in modulating and inducing a required behavior of cells on a substrate designed for biomedical applications, since an adequate level of surface wettability is capable to promote the cellular adhesion and proliferation through different cellular signaling pathways [39]. The high hydrophilic surface properties of hybrid HAG electrospun architecture (WCA = $26.0 \pm 1.13^{\circ}$) (Fig. 2, b) originated from the inherent hydrophilic properties of biopolymers of the matrix. The decoration with GO-COOH sheets slightly alter the apparent surface wettability of hybrid HAG/G electrospun architecture, the WCA is increased with approx.10° (WCA = 37.7 ± 1.84) and is correlated with the generally low intrinsic wettability of graphene, regardless of the presence of hydrophilic functionalities on the surface (e.g., COOH, OH) [40]. Unlike other coating materials, graphene is characterized by an unusual wettability behavior that is mainly impacted by its thinness (the number of layers) [41]. Rafiee et al. [42] have reported that a graphene monolayer does not alter the substrate wetting behavior and remains noninvasive to the substrate-water interface in the system where the van der Waals forces control the wetting (effect called "wetting transparency of graphene"), while increasing the number of graphene layers (n >6) determines a gradual transition towards high hydrophobic surface. Moreover, the Rafiee's team observed that the wetting transparency of graphene is destroyed on hydrophilic surfaces, where the substrate-water interface is dominated by short-range chemical forces (H-bonding with water) and the WCA gradually increases with respect to the growing number of graphene layers.

Further, we have investigated the *in vitro* degradation of hybrid electrospun architectures in the presence or absence of collagenase to evaluate the hydrolytic and enzymatic impact upon their stability (Fig. 2, c). In the presence of enzymes, the degradation process of all the investigated electrospun architectures is significantly accelerated and is attributable to high susceptibility of collagenase to degrade the protein backbone of samples [43]. The apparent weight-loss is approx. 2-Fold higher as compared to samples subjected to hydrolytic degradation (soaked only in PBS). Further, despite the hydrophobic character of graphene sheets, the structural integrity of hybrid HAG/G fibrous architecture disintegrates much rapidly upon both hydrolytic and enzymatic conditions, showing a high % mass-loss at each investigated time point when compared to that of HAG sample. Albeit it is well demonstrated the contribution of graphene in improving the scaffolds' resistance to degradation by altering the surface morphology and decelerating the water penetration rate within the internal matrix, the global stability of formulated biomaterials in different media is impacted by both polymer matrix and graphene features (e.g., structure, dispersion and interaction of graphene within the polymer matrix, nature of matrix). So, similar to unusual impact of graphene in reducing the global mechanical features of electrospun fibrous architectures, noted in our previous study [32], its presence might also accelerate the degradation process of materials through the generation of defects and cracks within the polymer matrix. This high internal porosity may facilitate the water permeation, leading to a faster disintegration of material through the bulk pathway, in accordance with other previously reported works [44,45].

4.1. PEI/pDNA nanoparticles design and characterization

The critical features in formulating efficient gene delivery systems mainly rely in achieving optimal hydrodynamic characteristics, stability and gene loading efficiency. The self-assembled PEI/pDNA Np are mainly formed owing to strong electrostatic interactions (charge attraction forces) as well as the small effects of thermal motions and translational or conformational entropy of chains [46] (Fig. 3, a). Therefore, the stability (zeta potential) and hydrodynamic features (mean hydrodynamic size and polydispersity) of PEI/pDNA Np are mainly dependent on the ratio of cationic PEI to anionic DNA (N/P). The amount of cationic charges from the system must be sufficient to stabilize the anionic compound inside the particles, as well as to ensure an appropriate peripheric stability of assembled nanoparticles, avoiding their agglomeration process. In this respect, we have investigated the degree of condensation of pDNA in the presence of PEI at three N/P ratios: 1, 4, 6 (Fig. 3b and c), selecting the complexation ratio that generates uniformly

distributed and robust PEI/pDNA Np.

It is noted that the N/P = 1 generates a broad bimodal size distributed population (PdI = 0.269 ± 0.015) with the largest mean hydrodynamic diameter of nanoparticles (d = 128.1 ± 1.2 nm). The hydrodynamic features are significantly improved when the N/P ratio is increased, leading to the formation of colloidal systems with d = 113.7 ± 1.6 nm and PdI = 0.104 ± 0.010 at N/P = 4 and d = 102.8 ± 1.2 nm and PdI = 0.125 ± 0.030 when the N/P = 6 is used (Supplementary Information, Fig. S1). The highly negative zeta potential (ζ = −44.3 ± 1.7 mV) of free pDNA is generated by the negatively charged phosphate functionalities (PO_4^{-3}); it becomes positively charged when a sufficient amount of polycation is added and the stable self-assembled nanoparticles are formed (N/P = 4, ζ = +27.7 ± 1.2 mV). The further addition of cationic polymer N/P = 6 does not impact the zeta value. On the contrary, if the amount of PEI is insufficient (N/P = 1), the zeta potential is modulated by the pDNA tracers (unbound pDNA) that are still in the system (ζ = −26.4 ± 1.0 mV) (Fig. 3, c). Considering that the surface cell membrane is negatively charged, the positively charged PEI/pDNA Np might promote the cellular uptake efficiency [47]. The generation of stable monomodal narrow distributed population of colloids at N/P = 4 is noted in DLS investigations and further in TEM micrographs, highlighting uniformly distributed nanoparticles with well-defined spherical shape (Fig. 3, d). So, to assure good stability and a consistent mean size of nanoparticles without triggering a significant cytotoxic response, which may arise at high PEI concentration [48] (SI, Fig. S2), the PEI/pDNA Np formulated at N/P = 4 are employed in further investigations.

4.2. Morphological features of formulated hybrid fibrous architectures

The difference in morphologies of as-spun and crosslinked hybrid HAG and HAG/G fibrous architectures are shown in Fig. 4a–d. SEM images substantiate smooth, homogeneous and continuous nanofiber morphology of hybrid HAG fibrous architecture that is not modified following the graphene dispersion (HAG/G). The morphology of post-crosslinked fibrous architecture is largely changed from continuous uniform nanofibers toward highly coiled ones, hardly recognizable in the case of hybrid HAG electrospun architecture and still well-defined in hybrid HAG/G counterpart. These conformational changes might be triggered by the two-step crosslinking that involved the use of glutaraldehyde vapor for protein stabilization, followed by the Ca^{2+} ionic gelation of polysaccharide backbone and the generation of egg box-like structures where other oxygen containing groups making scene in the system (e.g., COOH of protein or GO-COOH) may be also involved [49].

SEM micrographs of hybrid HAG-Np and HAG/G-Np fibrous architectures highlight the spherical PEI/pDNA nanoparticles distributed on the surface or integrated between the fibers (Fig. 4e and f). To further quantitate the extent of PEI/pDNA Np immobilized on the surface of hybrid fibrous architectures, as well as to determine the contribution of GO-COOH layers in this process, we have calculated the encapsulation efficiency (EE %) of both investigated fibrous structures. The calculated EE% after 2 h of scaffolds incubation in the presence of PEI/pDNA Np is 64.27 ± 0.16 % for HAG-Np and 69.07 ± 0.42 % for hybrid HAG/G-Np fibrous architectures. The preferential encapsulation of cationic PEI/pDNA Np on the surface of hybrid HAG/G scaffolds might be correlated with the graphene dispersion and the shift of surface potential toward high negative values, in accordance with SZP results. Comparable beneficial effect of graphene oxide (GO) incorporation in increasing the adsorption of PEI/pDNA onto PLGA/GO nanofibers was also noted by Wang et al. [50]. Besides, the extreme-large specific surface area of GO-COOH might also have a contribution in

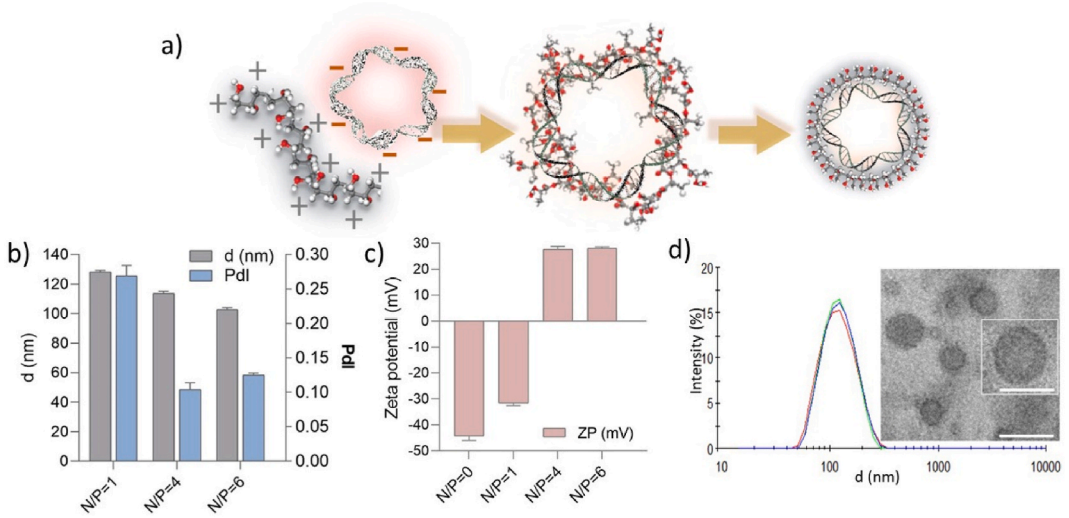

Fig. 3. Characterization of PEI/pDNA Np: **a) -** Self-assembling process of PEI/pDNA Np; **b) -** Mean hydrodynamic size (d, nm) and polydispersity (PdI) of PEI/pDNA Np at different N/P ratio; **c) –** Zeta potential (ζ, mV) measurements of PEI/pDNA Np. The positive ζ show the efficient encapsulation of negative pDNA with PEI, while the negative ζ shows the partial complexation of pDNA, as well as the insufficient amount of PEI to form stable self-assembled PEI/pDNA Np; **d)** – Size distribution graph and TEM micrograph of PEI/pDNA Np formulated at N/P = 4 (inset: scale bare 100 nm).

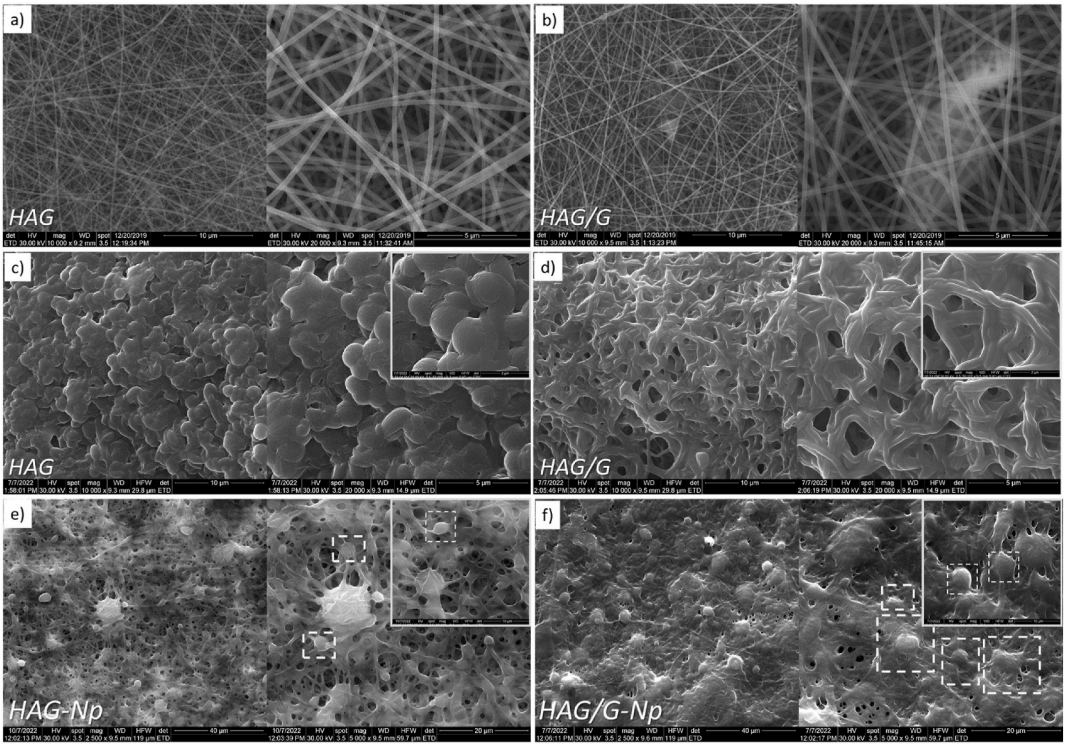

Fig. 4. Variation of morphological features of hybrid fibrous architectures: SEM micrographs of **a, b)** uncross-linked and **c, d)** crosslinked hybrid HAG and HAG/G fibrous architectures as well as **e, f)** hybrid fibrous architectures with PEI/pDNA Np immobilized on the surface (HAG-Np and HAG/G-Np). The fibrous structure of scaffolds is preserved following the crosslinking and PEI/pDNA Np immobilization regardless of the sample, while the amount of immobilized PEI/pDNA Np on their surface is different, prevailing onto hybrid HAG/G-Np fibrous architecture as compared to HAG-Np one.

enhancing the immobilization of PEI/pDNA Np by providing more absorption sites and through capturing some nanoparticles within the new formed pores of scaffold, as well [51]. Further, according to gel electrophoresis results (SI, Fig. 3) the integrity of PEI/pDNA Np was not impacted by the presence of GO-COOH which may also act as anionic competitor for PEI/pDNA Np during the immobilization process. This effect may be attributed to the high charge density of polycation and polyanion, along with the binding mode of PEI to DNA which imply strong electrostatic interactions and groove-binding effects [52] generating PEI/pDNA Np with superior stability as compared to the interactions between the PEI/pDNA and negatively charged functionalities distributed on the surface of hybrid electrospun architecture.

4.3. In vitro cell viability and cytotoxicity of hybrid fibrous architectures with surface immobilized PEI/pDNA Np

Cellular-level biocompatibility stands as a fundamental criterion for evaluating the quality of a biomaterial intended for clinical use. Cell viability and cytotoxicity tests represent pivotal components in the assessment of biocompatibility. Besides their excellent biocompatibility, the beneficial effect of biopolymers that form the matrix of electrospun architectures in sustaining cellular

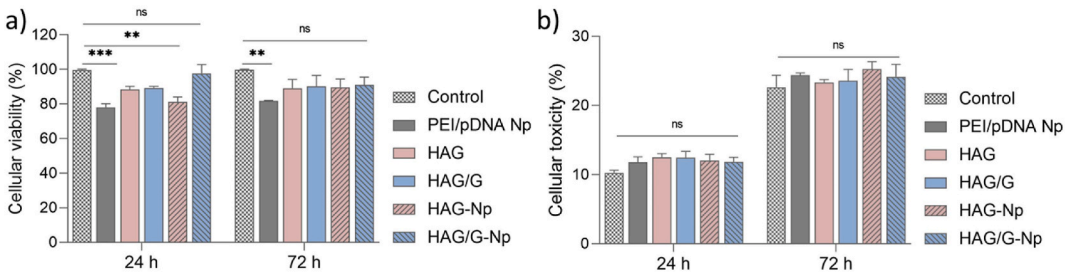

Fig. 5. Macrophages behavior in the presence of hybrid fibrous architectures with surface immobilized PEI/pDNA Np: **a)** metabolic (MTT assay) and **b)** cytotoxic (LDH assay) response after 24h and 72h of culture in standard conditions (Statistical significance: *ns* > *0.5;**p* < *0.01; ***p* < *0.001)*.

development, growth and proliferation is well reported in the literature. According to the abovementioned results (SZP, EE and degradation studies), the GO-COOH dispersion not only promotes the absorption of PEI/pDNA Np but also elicits the degradation of hybrid HAG/G fibrous architecture, which may improve the microenvironment and facilitate the cell development and growth.

As shown in Fig. 5 a, b after one day, the metabolic activity of macrophages seeded in the presence of investigated samples does not outperform that of the control sample, while the cytotoxic potential is comparable with the control, regardless of the investigated sample ($p > 0.5$). After 3 days of culture, the metabolic activity of macrophages is considerably improved, when comparing with the outcomes registered after one day, while the cytotoxic effect is insignificant ($p > 0.5$), suggesting a good biocompatibility and proliferation potency in all the tested biomaterials. However, among the investigated samples, PEI/pDNA Np presents the lowest ability to support cells proliferation and development regardless of the investigated time point, which may be correlated with some cytotoxicity associated with the intrinsic features of PEI [53] that might determine the plasma-membrane destabilization, cellular organelle damage, impairing cellular development [54]. The metabolic activity of cells is gradually improved when hybrid HAG and HAG/G fibrous architectures are tested. The highest proliferation potential of hybrid HAG-Np and HAG/G-Np electrospun architecture, comparable to control ($p > 0.5$) might be attributable to a decreased concentration of PEI/pDNA Np in the medium, owing to their gradual release from the electrospun substrates along with the microstructural characteristics of fibrous architectures and their

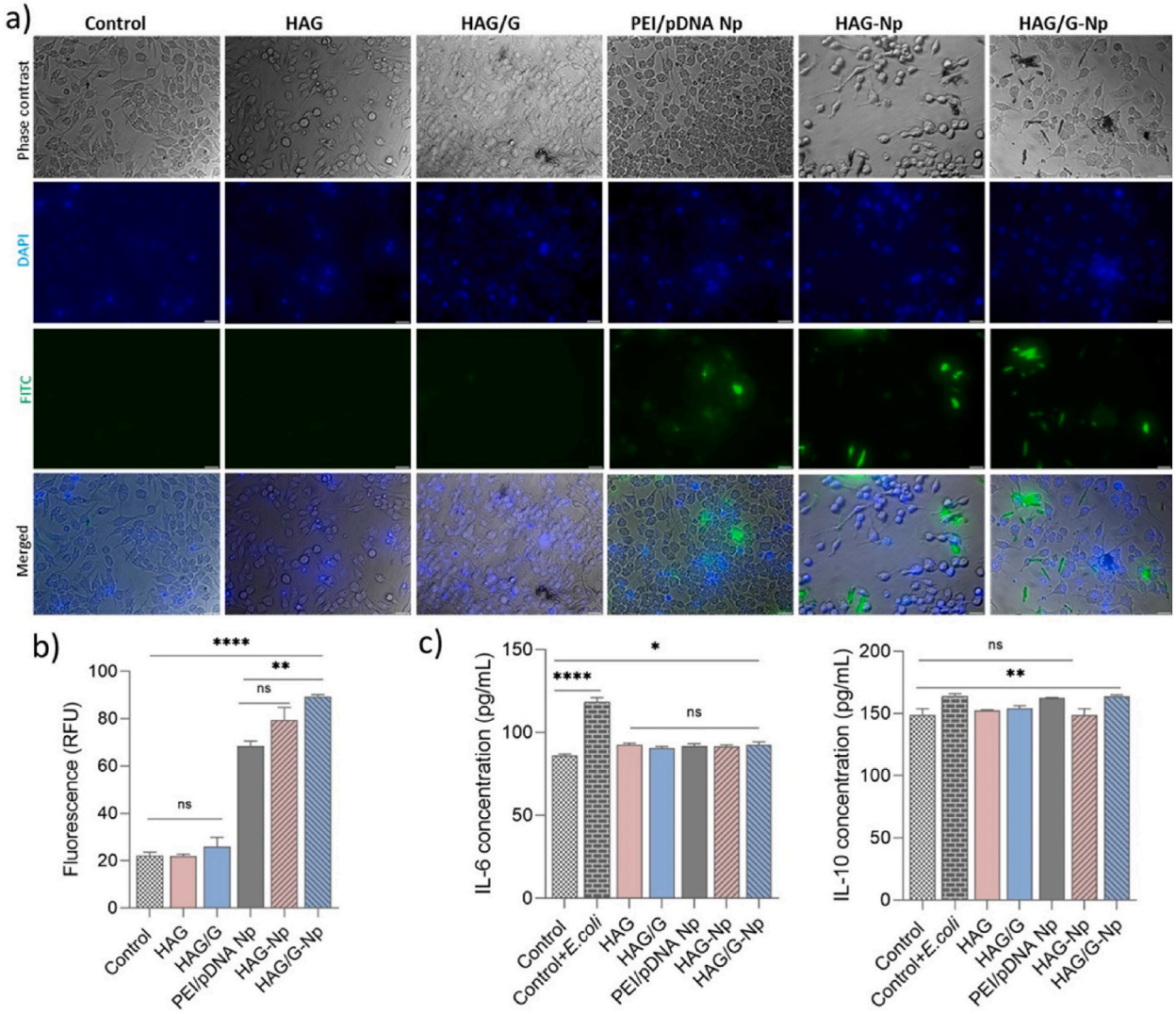

Fig. 6. *In vitro* biological activity of hybrid fibrous architectures with surface immobilized PEI/pDNA Np: **a**) Phase contrast and fluorescence microscopy of GFP expression in macrophages. After immobilizing PEI/pDNA Np on the surface of hybrid HAG and HAG/G electrospun architectures, RAW 264.7 macrophage cells were seeded and the expression of GFP was assessed after 24 h of transfection in standard culture condition. Cell nucleus was labeled with DAPI; Magnification 10× **b)** Quantification of GFP expression; **c)** Immunomodulatory profile of investigated biomaterials was evaluated by quantifying the level of IL-6 and IL-10 secreted by macrophages after 24 h of incubation in standard culture conditions (Statistical significance: *ns* > 0.5; *p < 0.05; **p < 0.01; ****p < 0.0001*).

similarity with the natural fibrillary extracellular matrix (ECM) [36,49]. Moreover, it is well-known that the surface functionalities of biomaterials are critical players in defining cellular behavior and toxicity. Zhang et al. [55] have done a comprehensive quantitative investigation on the relationship between mammalian cell behavior and surface properties of different polysaccharides bearing various functional groups wrapped onto single-wall carbon nanotubes. The author proved the direct contribution of –COOH, -OH and -NH_2 functionalities from the substrate in modulating the protein absorption, respectively cellular adhesion and proliferation.

4.4. In vitro biological activity of hybrid fibrous architectures with surface immobilized PEI/pDNA Np

The *in vitro* transient gene expression performances of PEI/pDNA Np immobilized onto hybrid electrospun architectures (HAG-Np and HAG/G-Np) were evaluated by fluorescent microscopy (Fig. 6a and b) and flow cytometry (SI, Fig. S4) using GFP as a reporter gene and monitoring the gene expression in RAW 264.7 macrophage cells 24 h post-transfection. We have also tested the fluorescent signal of cell culture seeded on hybrid HAG and HAG/G without Np to avoid any interferences.

It is worth mentioning that both, qualitative and quantitative fluorescent investigations show significant differences in transient gene expression between PEI/pDNA Np suspended in the medium and immobilized on the surface of the hybrid HAG-Np and HAG/G-Np electrospun architectures. Beside the absence of the fluorescent signal in the control and cells seeded on the hybrid HAG or HAG/G electrospun architectures, it is noted a considerably diminished gene expression in the case of cells incubated in the presence of free PEI/pDNA Np as compared to other GFP containing samples. According to the quantitative analyses, the minimal GFP expression is observed in PEI/pDNA Np sample (68.34 $\pm$ 2.19 RFU) and might be associated with the reduced ability of PEI/pDNA Np in supporting cells development observed in MTT analyses, along with the poor contact with cell membrane. The immobilization of PEI/pDNA Np on the surface of hybrid electrospun architectures increases the gene transfection to 79.44 $\pm$ 2.19 RFU when the macrophages are seeded on HAG-Np and the highest transient gene expression is observed for hybrid HAG/G-Np electrospun architectures (89.71 $\pm$ 0.86 RFU). Further, the flow cytometry analyses show that the mean fluorescence signal is gradually progressing with respect to the investigated sample in the following order: the lowest signal is registered in the PEI/pDNA Np sample, following by HAG-Np, and the highest GFP expression is noted in hybrid HAG/G-Np sample 24 h post-transfection (SI, Fig. S4), in line with fluorescent investigations. These results suggest that the hybrid HAG/G-Np elecrospun architectures are important contributors in the efficient gene transfection process, acting as substrate for nanoparticles, are capable not only to locally deliver the loaded cargo but also to ensure a direct contact with cells, fostering their cellular internalization. It is well documented that the cellular internalization process is mainly driven by the endocytosis mechanism and the type of interactions that occur between cellular membrane and positively or negatively charged carriers [56,57]. Usually, cationic carriers are prone to a better internalization level owing to electrostatic interaction with the negatively charged cell membrane, supplementary having a contribution in the endosomal escape and intracellular trafficking [10]. In comparison with HAG-Np sample, the GFP expression is slightly higher in HAG/G-Np and these differences may be ascribed: firstly, to the amount of PEI/pDNA Np immobilized on the two substrates (in accordance with EE results) and secondly, to the surface topography of hybrid HAG/G electrospun architecture [58]. For instance, Muniyandi et al. [59] have explored the potency of PLLA electrospun scaffolds with different topologies (coated or not with fibronectin) in improving direct reprogramming of adult human cardiac fibroblasts. The authors have noted an important contribution of fibronectin functionalization in improving the loading efficiency of PEI-miRNA polyplexes and further in advancing the cellular uptake and respectively the reprograming efficiency. In another work, Pankongadisak and collaborators [60] have managed to increase the gene transfection efficiency of pDNA polyplexes from gelatin fiber mats through the addition of PEG, which improved the pDNA encapsulation efficiency.

Beside the biocompatibility and transient gene transfection, another important aspect relies in the evaluation of the immune response of macrophages against the investigated biomaterials.

It is acknowledged that macrophages are effector cells of immune systems that fulfil crucial functions in homeostasis and in disease by releasing both pro-inflammatory (e.g., IL-6, IL-12, THF-α) or anti-inflammatory cytokines (e.g., IL-10, TGF-β) [61]. Therefore, we evaluated the immunomodulatory behavior of biomaterials on two markers, the proinflammatory IL-6 and anti-inflammatory IL-10 cytokines (Fig. 6, c). Interestingly, after 24 h no release of proinflammatory IL-6 is observed against any investigated sample, the amount of released IL-6 cytokine is comparable to unstimulated macrophages (control), while in the case of *E. coli* stimulated cellular culture (control + *E. coli*) a significant release of proinflammatory marker is noted. On the other hand, no significant differences are noted in the level of anti-inflammatory IL-10 marker released, when RAW 264.7 macrophage cells are treated with the investigated samples. According to the results, only free PEI/pDNA Np and hybrid HAG/G-Np electrospun architecture are able to slightly trigger some anti-inflammatory responses in cultured cells as compared to control ($p < 0.01$). The effect of surface charge polarity of biomaterials (negative or positive charges) on cellular behavior and responses has been controversially discussed. In a previous report, Usman et al. [62] have demonstrated that the negatively charged carbon dots modified with citric acid foster a quite higher macrophage uptake and do not induce any inflammatory responses as compared to positively charged counterparts that present a concentration dependent increase in pro-inflammatory released markers. Conversely, Panariti and team [63] have revealed that in the interaction with immune cells, positively charged substrates are more susceptible to macrophage internalization, owing to negatively charged cell membrane, in comparison to negative or neutral particles. In another work, Chen and Gao [64] have noted that ovalbumin-coated gold nanoparticles, because of the high negative surface charge, are prone to induce higher inflammatory reaction in RAW246.7 macrophages cultured *in vitro* as compared to less negative PEG-coated nanoparticles.

5. Conclusion

The bioinspired electrospun fibrous architecture – mediated delivery of gene is highly suited for biomedical applications, owing to

their versatility, biomimicry and ability to release the cargo in a spatio-temporal dynamic, improving the therapeutic outcomes. In this work, hybrid electrospun architecture decorated with GO-COOH for *in vitro* local and controlled delivery of PEI/pDNA Np as an alternative to systemic gene delivery carriers to macrophages were reported. The PEI/pDNA Np were formed through electrostatic interactions, using different N/P ratios and hydrodynamic and morphological studies (DLS, TEM) showed the assembly of monomodal distributed colloidal population (PdI = 0.125) with the nanometric size (d∼100 nm), good stability (ζ∼+27 mV) and well-defined spherical shape at N/P = 4. Since the immobilization of positively charged PEI/pDNA Np on the surface of hybrid fibrous architectures was mainly driven by electrostatic interactions, we hypothesized that the loading efficiency of nanoparticles could be tuned by modulating the amount of negatively charged functionalities within the hybrid electrospun architectures through the dispersion of GO-COOH sheets. The dispersion of GO-COOH sheets shifted the surface charge of hybrid electrospun architectures to higher negative values with∼4 units (SZP analyses), up to 1.5-fold increased the apparent surface wettability (WCA measurements) as well as accelerated the *in vitro* degradation process. At the same time, the presence of GO-COOH increased the amount of immobilized nanoparticles onto the surface of hybrid electrospun architectures (EE = 64.27 % for HAG and 69.07 % for HAG/G). Alongside the fibrous structure of hybrid electrospun architectures, SEM micrographs highlighted very well the presence of PEI/pDNA Np that were distributed onto the surface of scaffolds or integrated between the fibers. Biological investigations showed that the hybrid electrospun architectures, beside the good biocompatibility and proliferation potential (MTT), were capable to promote the cellular internalization of PEI/pDNA Np immobilized on the surface, through insuring a direct contact with cells.

Further investigations on the *in vitro* biological behavior of the formulated hybrid electrospun architectures decorated with GO-COOH are foreseen to guarantee the therapeutic efficiency and safety of the proposed systems as efficient substrates for local delivery of PEI/pDNA Np in advanced gene therapy.

Data availability statement

Data will be made available on request. Data were not deposited into a publicly available repository.

CRediT authorship contribution statement

Jana Ghitman: Writing – review & editing, Writing – original draft, Methodology, Investigation, Formal analysis, Conceptualization. **Gratiela Gradisteanu Pircalabioru:** Writing – original draft, Methodology, Investigation. **Calin Deleanu:** Visualization, Methodology, Investigation. **Eugeniu Vasile:** Methodology, Investigation. **Ciprian Iliescu:** Writing – review & editing, Visualization. **Horia Iovu:** Writing – review & editing, Validation, Supervision, Funding acquisition.

Declaration of competing interest

The authors declare no conflict of interest.

Acknowledgement

This work was supported by a grant from the Ministry of Research Innovation and Digitization, CNCS/CCCDI – UEFISCDI, project no. PN-III-P1-1.1-PD-2019-0205 (contract no. PD 83/2020), within PNCDI III. The DLS, Surface Zeta Potential and Water Contact Angle measurements were possible due to European Regional Development Fund through Competitiveness Operational Program 2014–2020, Priority axis 1, ID P_36_611, MySMIS code 107066, INOVABIOMED.

JG, GG, CI, HI acknowledge the European Union's Horizon Europe Research and Innovation framework programme 2021–2027, under the Coordination and Support Actions, HORIZON-WIDERA-2022-TALENTS-01 (grant agreement - 101087007 – eBio-hub). Funded by the European Union. Views and opinions expressed are however those of the author(s) only and do not necessarily reflect those of the European Union or European Research Executive Agency (REA). Neither the European Union nor the granting authority can be held responsible for them.

Appendix A. Supplementary data

Supplementary data to this article can be found online at https://doi.org/10.1016/j.heliyon.2024.e38071.

References

[1] https://www.prnewswire.com/news-releases/global-cell-and-gene-therapy-market-expected-to-grow-at-26-4-cagr-reaching-23-3-billion-by-2028–302172916.html. (Accessed 18 June 2024).
[2] H. Yin, R.L. Kanasty, A.A. Eltoukhy, A.J. Vegas, J.R. Dorkin, D.G. Anderson, Non-viral vectors for gene-based therapy, Nat. Rev. Genet. 15 (8) (2014) 541–555.
[3] J.T. Bulcha, Y. Wang, H. Ma, P.W. Tai, G. Gao, Viral vector platforms within the gene therapy landscape, Signal Transduct. Targeted Ther. 6 (1) (2021) 53.
[4] M.J. Mitchell, M.M. Billingsley, R.M. Haley, M.E. Wechsler, N.A. Peppas, R. Langer, Engineering precision nanoparticles for drug delivery, Nat. Rev. Drug Discov. 20 (2) (2021) 101–124.
[5] K. Paunovska, D. Loughrey, J.E. Dahlman, Drug delivery systems for RNA therapeutics, Nat. Rev. Genet. 23 (5) (2022) 265–280.

[6] M.P. Stewart, A. Sharei, X. Ding, G. Sahay, R. Langer, K.F. Jensen, In vitro and ex vivo strategies for intracellular delivery, Nature 538 (7624) (2016) 183–192.
[7] C.E. Thomas, A. Ehrhardt, M.A. Kay, Progress and problems with the use of viral vectors for gene therapy, Nat. Rev. Genet. 4 (5) (2003) 346–358.
[8] M. Mehta, T.A. Bui, X. Yang, Y. Aksoy, E.M. Goldys, W. Deng, Lipid-based nanoparticles for drug/gene delivery: an overview of the production techniques and difficulties encountered in their industrial development, ACS Materials Au 3 (6) (2023) 600–619.
[9] R. Mashima, S. Takada, Lipid nanoparticles: a novel gene delivery technique for clinical application, Curr. Issues Mol. Biol. 44 (10) (2022) 5013–5027.
[10] X. Hou, T. Zaks, R. Langer, Y. Dong, Lipid nanoparticles for mRNA delivery, Nat. Rev. Mater. 6 (12) (2021) 1078–1094.
[11] D. Pozzi, G. Caracciolo, Looking back, moving forward: lipid nanoparticles as a promising frontier in gene delivery, ACS Pharmacol. Transl. Sci. 6 (11) (2023) 1561–1573.
[12] A. Akinc, M.A. Maier, M. Manoharan, K. Fitzgerald, M. Jayaraman, S. Barros, P.R. Cullis, The Onpattro story and the clinical translation of nanomedicines containing nucleic acid-based drugs, Nat. Nanotechnol. 14 (12) (2019) 1084–1087.
[13] L.R. Baden, et al., Efficacy and safety of the mRNA-1273 SARS-CoV-2 vaccine, N. Engl. J. Med. 384 (2021) 403–416.
[14] J. Jiang, J. Mei, Y. Ma, S. Jiang, J. Zhang, S. Yi, Y. Liu, Tumor hijacks macrophages and microbiota through extracellular vesicles, Explorations 2 (1) (2022, February) 20210144.
[15] I.K. Herrmann, M.J.A. Wood, G. Fuhrmann, Extracellular vesicles as a next-generation drug delivery platform, Nat. Nanotechnol. 16 (7) (2021) 748–759.
[16] E. Tzng, N. Bayardo, P.C. Yang, Current challenges surrounding exosome treatments, Extracellular Vesicle 2 (2023) 100023.
[17] H.I. Kim, J. Park, Y. Zhu, X. Wang, Y. Han, D. Zhang, Recent advances in extracellular vesicles for therapeutic cargo delivery, Exp. Mol. Med. 56 (4) (2024) 836–849.
[18] R. Cecchin, Z. Troyer, K. Witwer, K.V. Morris, Extracellular vesicles: the next generation in gene therapy delivery, Mol. Ther. 31 (5) (2023) 1225–1230.
[19] K.D. Popowski, B.L. de Juan Abad, A. George, D. Silkstone, E. Belcher, J. Chung, K. Cheng, Inhalable exosomes outperform liposomes as mRNA and protein drug carriers to the lung, Extracellular Vesicle 1 (2022) 100002.
[20] E. Cojocaru, J. Ghitman, R. Stan, Electrospun-fibrous-architecture-mediated non-viral gene therapy drug delivery in regenerative medicine, Polymers 14 (13) (2022) 2647.
[21] S. Lee, G. Jin, J.H. Jang, Electrospun nanofibers as versatile interfaces for efficient gene delivery, J. Biol. Eng. 8 (1) (2014) 1–19.
[22] Y. Lavin, A. Mortha, A. Rahman, M. Merad, Regulation of macrophage development and function in peripheral tissues, Nat. Rev. Immunol. 15 (12) (2015) 731–744.
[23] Y. Zheng, Y. Han, Q. Sun, Z. Li, Harnessing anti-tumor and tumor-tropism functions of macrophages via nanotechnology for tumor immunotherapy, Explorations 2 (3) (2022, June) 20210166.
[24] Y.R. Na, S.W. Kim, S.H. Seok, A new era of macrophage-based cell therapy, Exp. Mol. Med. 55 (9) (2023) 1945–1954.
[25] A.S. Poltavets, P.A. Vishnyakova, A.V. Elchaninov, G.T. Sukhikh, T.K. Fatkhudinov, Macrophage modification strategies for efficient cell therapy, Cells 9 (6) (2020) 1535.
[26] D.L. Puhl, D. Mohanraj, D.W. Nelson, R.J. Gilbert, Designing electrospun fiber platforms for efficient delivery of genetic material and genome editing tools, Adv. Drug Deliv. Rev. (2022) 114161.
[27] S.Y. Lee, J. Fierro Jr, J. Dipasquale, A. Bastian, A.M. Tran, D. Hong, H. Dou, Engineering human circulating monocytes/macrophages by systemic deliverable gene editing, Front. Immunol. 13 (2022).
[28] K. Kawabata, Y. Takakura, M. Hashida, The fate of plasmid DNA after intravenous injection in mice: involvement of scavenger receptors in its hepatic uptake, Pharmaceut. Res. 12 (1995) 825–830.
[29] S. Mahor, B.C. Dash, S. O'Connor, A. Pandit, Mannosylated polyethyleneimine–hyaluronan nanohybrids for targeted gene delivery to macrophage-like cell lines, Bioconjugate Chem. 23 (6) (2012) 1138–1148.
[30] Y. Zhang, Y. Wang, C. Zhang, J. Wang, D. Pan, J. Liu, F. Feng, Targeted gene delivery to macrophages by biodegradable star-shaped polymers, ACS Appl. Mater. Interfaces 8 (6) (2016) 3719–3724.
[31] B. Burke, S. Sumner, N. Maitland, C.E. Lewis, Macrophages in gene therapy: cellular delivery vehicles and in vivo targets, J. Leukoc. Biol. 72 (3) (2002) 417–428.
[32] J. Ghitman, E.I. Biru, E. Cojocaru, G.G. Pircalabioru, E. Vasile, H. Iovu, Design of new bioinspired GO-COOH decorated alginate/gelatin hybrid scaffolds with nanofibrous architecture: structural, mechanical and biological investigations, RSC Adv. 11 (22) (2021) 13653–13665.
[33] Z. Dai, C. Wu, How does DNA complex with polyethylenimine with different chain lengths and topologies in their aqueous solution mixtures? Macromolecules 45 (10) (2012) 4346–4353.
[34] S. Bhattacharjee, DLS and zeta potential–what they are and what they are not? J. Contr. Release 235 (2016) 337–351.
[35] S. Kaja, A.J. Payne, Y. Naumchuk, P. Koulen, Quantification of lactate dehydrogenase for cell viability testing using cell lines and primary cultured astrocytes, Current protocols in toxicology 72 (1) (2017) 2–26.
[36] A. Luraghi, F. Peri, L. Moroni, Electrospinning for drug delivery applications: a review, J. Contr. Release 334 (2021) 463–484.
[37] S. Metwally, S. Ferraris, S. Spriano, Z.J. Krysiak, Ł. Kaniuk, M.M. Marzec, U. Stachewicz, Surface potential and roughness controlled cell adhesion and collagen formation in electrospun PCL fibers for bone regeneration, Mater. Des. 194 (2020) 108915.
[38] J.C. Courtenay, M.A. Johns, F. Galembeck, C. Deneke, E.M. Lanzoni, C.A. Costa, R.I. Sharma, Surface modified cellulose scaffolds for tissue engineering, Cellulose 24 (1) (2017) 253–267.
[39] X. Zhang, L. Meng, Q. Lu, Cell behaviors on polysaccharide-wrapped single-wall carbon nanotubes: a quantitative study of the surface properties of biomimetic nanofibrous scaffolds, ACS Nano 3 (10) (2009) 3200–3206.
[40] L.A. Belyaeva, G.F. Schneider, Wettability of graphene, Surf. Sci. Rep. 75 (2) (2020) 100482.
[41] D. Kim, E. Kim, S. Park, S. Kim, B.K. Min, H.J. Yoon, M. Cho, Wettability of graphene and interfacial water structure, Chem 7 (6) (2021) 1602–1614.
[42] J. Rafiee, X. Mi, H. Gullapalli, A.V. Thomas, F. Yavari, Y. Shi, N.A. Koratkar, Wetting transparency of graphene, Nat. Mater. 11 (3) (2012) 217–222.
[43] S. Suvarnapathaki, M.A. Nguyen, X. Wu, S.P. Nukavarapu, G. Camci-Unal, Synthesis and characterization of photocrosslinkable hydrogels from bovine skin gelatin, RSC Adv. 9 (23) (2019) 13016–13025.
[44] S. Sánchez-González, N. Diban, A. Urtiaga, Hydrolytic degradation and mechanical stability of poly (ε-Caprolactone)/reduced graphene oxide membranes as scaffolds for in vitro neural tissue regeneration, Membranes 8 (1) (2018) 12.
[45] T.X. Jin, C. Liu, M. Zhou, S.G. Chai, F. Chen, Q. Fu, Crystallization, mechanical performance and hydrolytic degradation of poly (butylene succinate)/graphene oxide nanocomposites obtained via in situ polymerization, Compos. Appl. Sci. Manuf. 68 (2015) 193–201.
[46] V. Mengarelli, L. Auvray, D. Pastré, M. Zeghal, Charge inversion, condensation and decondensation of DNA and polystyrene sulfonate by polyethylenimine, The European Physical Journal E 34 (11) (2011) 1–10.
[47] M. Wen, F. Zhou, C. Cui, Y. Zhao, X. Yuan, Performance of TMC-g-PEG-VAPG/miRNA-145 complexes in electrospun membranes for target-regulating vascular SMCs, Colloids Surf. B Biointerfaces 182 (2019) 110369.
[48] S.M. Moghimi, P. Symonds, J.C. Murray, A.C. Hunter, G. Debska, A. Szewczyk, A two-stage poly (ethylenimine)-mediated cytotoxicity: implications for gene transfer/therapy, Mol. Ther. 11 (6) (2005) 990–995.
[49] S. Park, K.S. Lee, G. Bozoklu, W. Cai, S.T. Nguyen, R.S. Ruoff, Graphene oxide papers modified by divalent ions—enhancing mechanical properties via chemical cross-linking, ACS Nano 2 (3) (2008) 572–578.
[50] Z. Wang, H. Shen, S. Song, L. Zhang, W. Chen, J. Dai, Z. Zhang, Graphene oxide incorporated PLGA nanofibrous scaffold for solid phase gene delivery into mesenchymal stem cells, J. Nanosci. Nanotechnol. 18 (4) (2018) 2286–2293.
[51] W. Li, D. Wu, S. Zhu, Z. Liu, B. Luo, L. Lu, C. Zhou, Sustained release of plasmid DNA from PLLA/POSS nanofibers for angiogenic therapy, Chem. Eng. J. 365 (2019) 270–281.
[52] K. Utsuno, H. Uludağ, Thermodynamics of polyethylenimine-DNA binding and DNA condensation, Biophys. J. 99 (1) (2010) 201–207.
[53] V. Kafil, Y. Omidi, Cytotoxic impacts of linear and branched polyethylenimine nanostructures in a431 cells, Bioimpacts: BI 1 (1) (2011) 23.

[54] S. He, J. Fang, C. Zhong, F. Ren, M. Wang, Controlled pVEGF delivery via a gene-activated matrix comprised of a peptide-modified non-viral vector and a nanofibrous scaffold for skin wound healing, Acta Biomater. 140 (2022) 149–162.
[55] X. Zhang, L. Meng, Q. Lu, Cell behaviors on polysaccharide-wrapped single-wall carbon nanotubes: a quantitative study of the surface properties of biomimetic nanofibrous scaffolds, ACS Nano 3 (10) (2009) 3200–3206.
[56] S. Salatin, A. Yari Khosroushahi, Overviews on the cellular uptake mechanism of polysaccharide colloidal nanoparticles, J. Cell Mol. Med. 21 (9) (2017) 1668–1686.
[57] D. Zhang, L. Wei, M. Zhong, L. Xiao, H.W. Li, J. Wang, The morphology and surface charge-dependent cellular uptake efficiency of upconversion nanostructures revealed by single-particle optical microscopy, Chem. Sci. 9 (23) (2018) 5260–5269.
[58] C. Huang, T. Ozdemir, L.C. Xu, P.J. Butler, C.A. Siedlecki, J.L. Brown, S. Zhang, The role of substrate topography on the cellular uptake of nanoparticles, J. Biomed. Mater. Res. B Appl. Biomater. 104 (3) (2016) 488–495.
[59] P. Muniyandi, V. Palaninathan, T. Mizuki, M.S. Mohamed, T. Hanajiri, T. Maekawa, Scaffold mediated delivery of dual miRNAs to transdifferentiate cardiac fibroblasts, Mater. Sci. Eng. C 128 (2021) 112323.
[60] P. Pankongadisak, E. Tsekoura, O. Suwantong, H. Uludağ, Electrospun gelatin matrices with bioactive pDNA polyplexes, Int. J. Biol. Macromol. 149 (2020) 296–308.
[61] C. Zhang, M. Yang, A.C. Ericsson, Function of macrophages in disease: current understanding on molecular mechanisms, Front. Immunol. 12 (2021) 620510.
[62] M. Usman, Y. Zaheer, M.R. Younis, R.E. Demirdogen, S.Z. Hussain, Y. Sarwar, A. Ihsan, The effect of surface charge on cellular uptake and inflammatory behavior of carbon dots, Colloid and Interface Science Communications 35 (2020) 100243.
[63] A. Panariti, G. Miserocchi, I. Rivolta, The effect of nanoparticle uptake on cellular behavior: disrupting or enabling functions? Nanotechnol. Sci. Appl. (2012) 87–100.
[64] X. Chen, C. Gao, Influences of size and surface coating of gold nanoparticles on inflammatory activation of macrophages, Colloids Surf. B Biointerfaces 160 (2017) 372–380.